Supporting Information for:

Regulation of luminescence band and exploration of antibacterial activity of a nanohybrid composed of flurophore-phenothiazine nanoribbons dispersed with Ag nanoparticles

Lin Kong, Jia-xiang Yang, Zhao-Ming Xue, Hong-ping Zhou, Long-jiu Cheng,

Qiong Zhang, Jie-ying Wu, Bao-kang Jin, Sheng-Yi Zhang, Yu-peng Tian

Contents:

Preparation of Intermediate 1: 10-Ethyl-10H-phenothiazine-3-carbaldehyde was prepared in our laboratory previously [S1]. To synthesize Intermediate 1, 10-Ethyl-10H- phenothiazine-3-carbaldehyde (0.51 g, 2 mmol) was dissolved in 20 mL methanol, $NaBH_4$ (0.19 g, 5 mmoL) was added in batches. After the solution was stirred for 6 h, methanol was evaporated to get intermediate **1** as a white solid. ^{1}H NMR (400 MHz, d_6-DMSO) δ(ppm): 7.18 (t, 1H, J = 8.0 Hz); 7.11 (t, 1H, J = 7.6 Hz); 7.07 (s, 1H); 6.99 (d, 2H, J = 8.4 Hz); 6.95 (d, 1H, J = 8.0 Hz); 6.91 (t, 1H, J = 7.2 Hz); 5.09 (s, 1H); 4.38 (s, 2H); 3.89 (m, 2H); 1.28 (t, 3H, J = 6.8 Hz). ^{13}C NMR (100 MHz, d_6-DMSO) δ(ppm): 149.76, 148.18, 141.96, 132.80, 132.20, 131.11, 130.47, 128.08, 127.90, 127.42, 120.52, 120.32, 67.32, 46.26, 17.88.

Then, intermediate **2** (0.26 g, 1 mmol), triphenylphosphine (0.31 g, 1.2 mmol) were dissolved in $CHCl_3$ (30 mL), then, KI solution (0.25 g, 1.5 mmol, dissolved in 1 mL water), glacial acetic acid (5 mL) and little 18-C-6 were added to the above $CHCl_3$ solution. The as-prepared solution was stirred for one week. The reaction was monitored by TLC to ensure complete reaction. Then, the solvent was removed with a rotary evaporator. The residue was then washed with dimethylbenzene to obtain 0.61 g intermediate **2** as a light yellow solid (95% in yield).
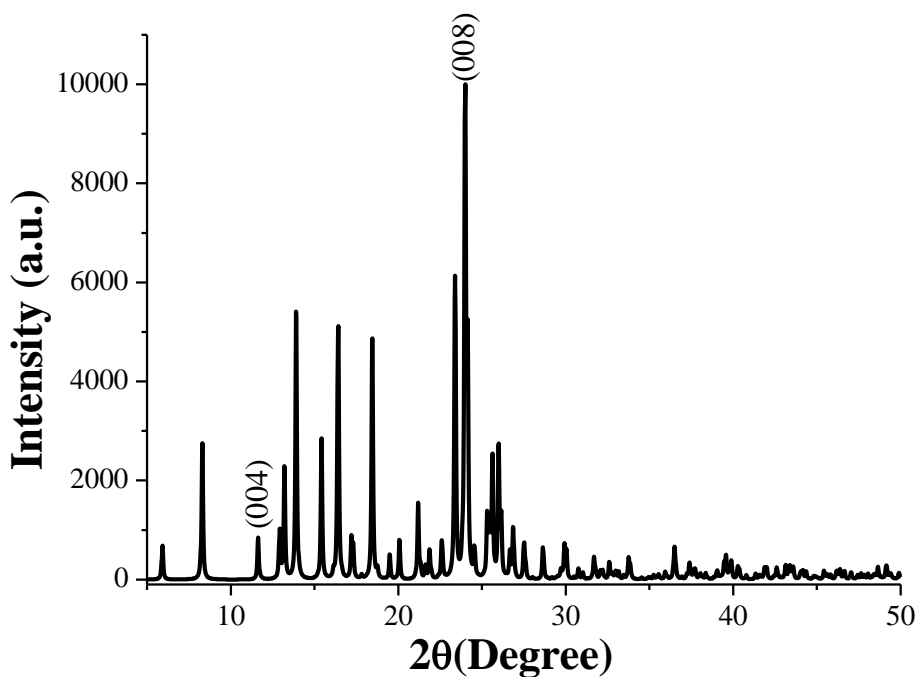
Fig. S1 XRD patterns of **L** single crystal

Table S1. Bond lengths [Å] and angles [°] for **L**

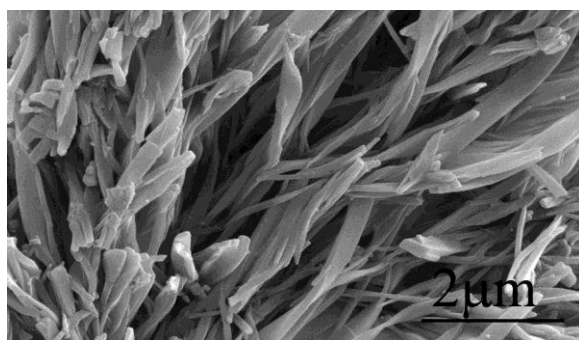|					
C(1)-C(2)	1.386(4)	S(1)–C(1)	1.760(3)	C(6)–N(1)	1.416(4)
C(1)-C(6)	1.403(4)	C(7)-N(1)	1.410(4)	C(13)-N(1)	1.467(3)
C(7)-C(12)	1.405(4)	C(10)-C(15)	1.491(5)	C(15)-C(16)	1.295(4)
C(16)-C(17)	1.477(5)	C(17)-C(18)	1.377(4)	C(20)-C(23)	1.461(5)
C(23)-O(1)	1.213(4)	C(2)-H(2)	0.9300		
C(2)-C(1)-S(1)	120.6(2)	C(3)-C(2)-C(1)	120.4(3)	C(1)-S(1)-C(12)	97.76(15)
C(7)-N(1)-C(6)	117.8(2)	O(1)-C(23)-C(20)	125.4(4)	C(8)-C(7)-N(1)	124.2(3)
C(16)-C(15)-C(10)	128.1(3)	C(15)-C(16)-C(17)	124.6(4)	C(19)-C(20)-C(23)	120.1(3)

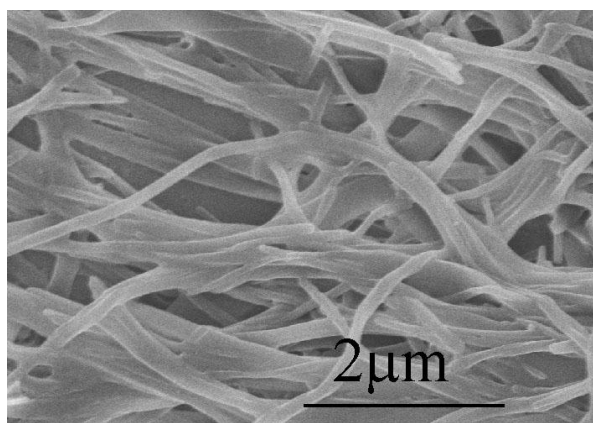**Fig. S2** SEM of **L** nanoribbons obtained from THF-H_2O solution

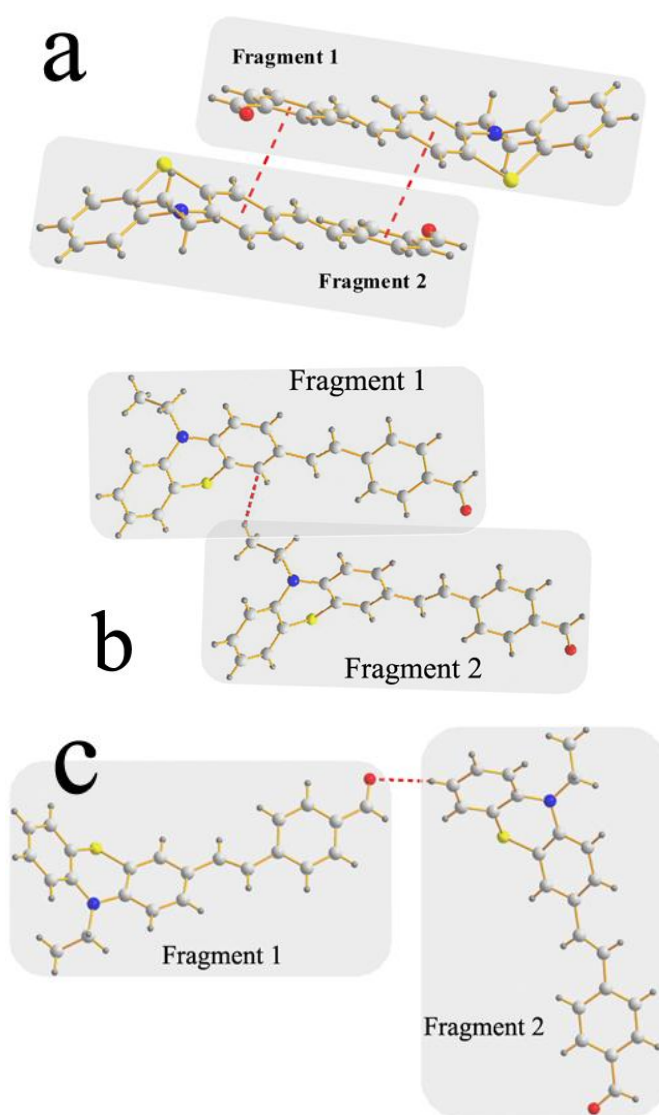**Fig. S3** SEM of **L** nanoribbons obtained from EtOH-H$_2$O solution

Fig. **S4**. Fragments selected for weak interactions along: (a) *a* axis, (b) *b* axis, (c) *c* axis.

Table S2 Calculated excitation energies (E), oscillator strengths (f), corresponding wavelengths (λ_{abs}) and major contributors for **L**

Comp.	E(eV)	λ_{abs}(nm)	f	Nature of Transitions
L	3.0849	401.90	0.3491	HOMO→LUMO
	3.9107	317.04	0.5140	HOMO-1→LUMO
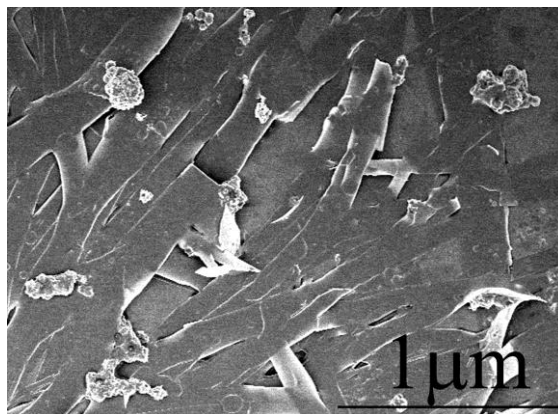
Fig. S5 SEM micrograph of the mixture physically mixed **L** nanoribbons and Ag NCs
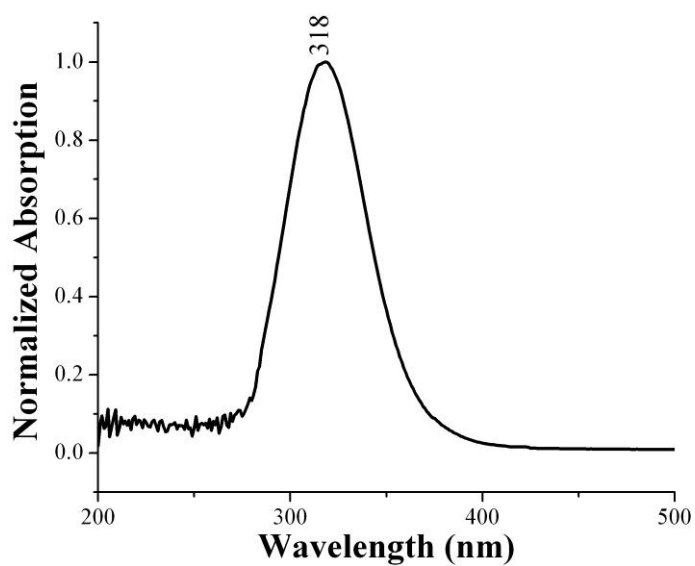

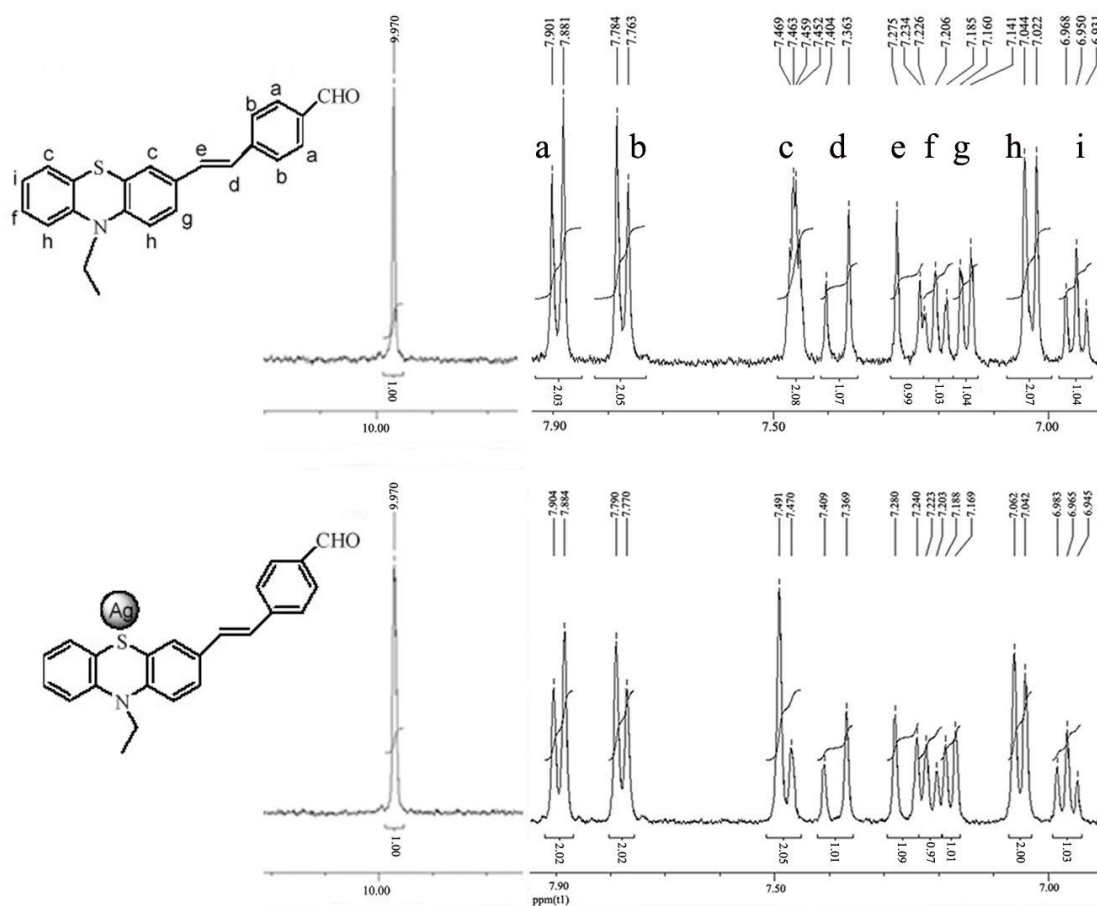**Fig. S6** UV-Vis spectrum of phenothiazine fragment

Fig. S7 A comparison of ^{1}H-NMR spectrum of **L** and **L**/Ag nanohybrid
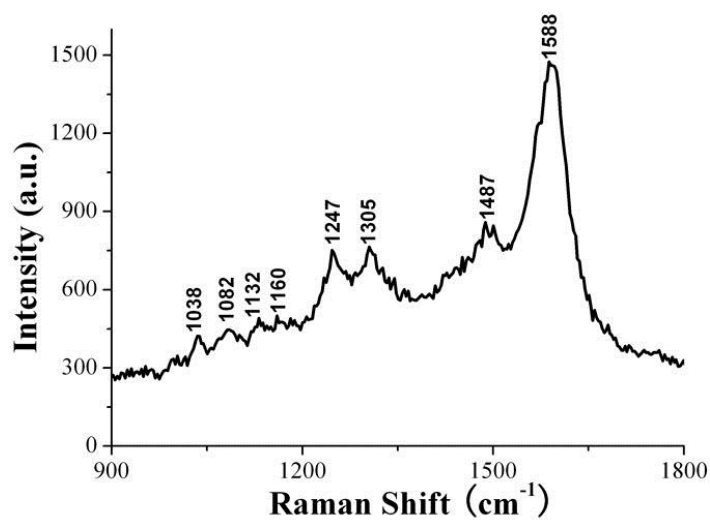

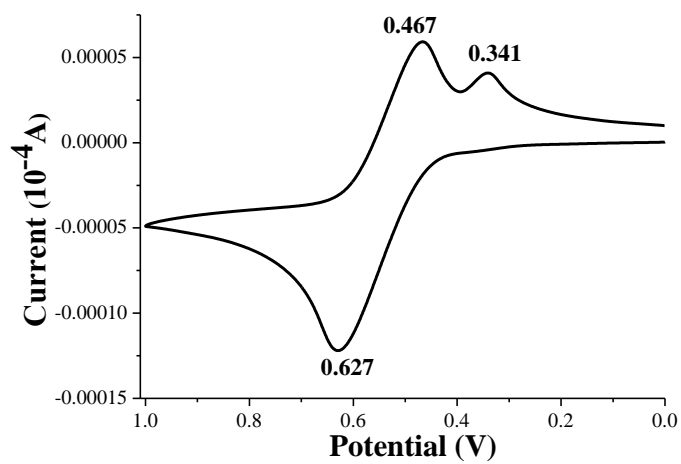**Fig. S8** Raman spectrum of phenothiazine fragment

Fig. S9 Cyclic-voltammetric response of phenothiazine fragement
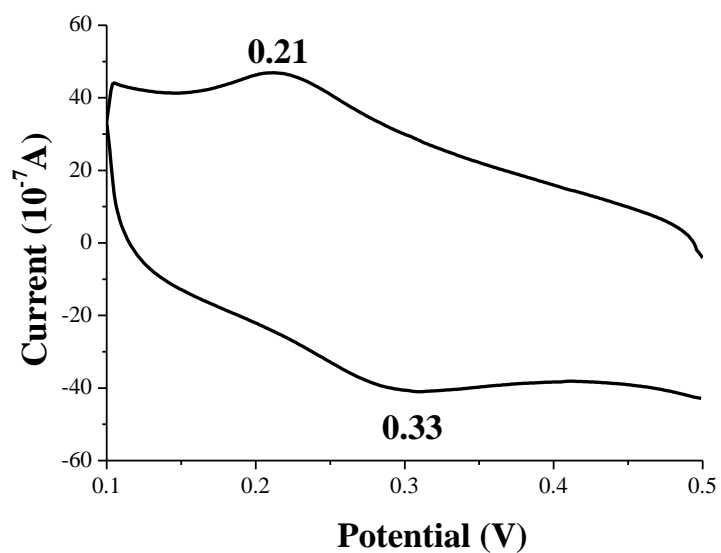

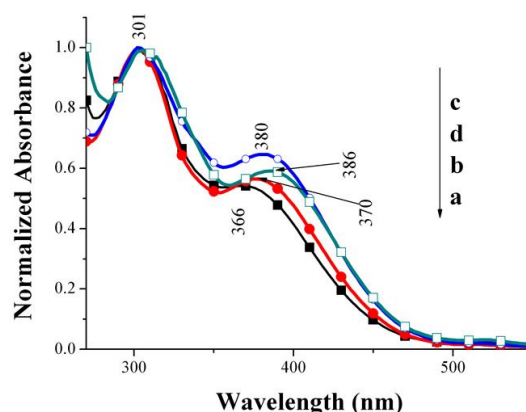**Fig. S10** Cyclic-voltammetric response of AgNO$_3$

Figure S11 UV-vis spectra of **L**/Ag nanohybrids prepared with different molar ratio of **L** to Ag

(a) 1**L**:10Ag; (b) 1**L**:1Ag; (c) 2**L**:1Ag; (d) 5**L**:1Ag.

Effect of concentration of AgNO$_3$ on the formation of the nanohybrid

It was found that the number of Ag NPs attaching on **L** nanoribbons was also depended on the concentration of AgNO$_3$. When the usage of AgNO$_3$ was very few, only a small amount of Ag NPs scattered in distribution on the surface of **L** nanoribbons (as shown in Fig. S12-a and -b). As the usage of AgNO$_3$ increased, the number of Ag NPs clinging to **L** ribbons increased along with it (**Fig. S12-c to -f**), and Ag NPs tended to aggregate more and more at the same time. It can also be seen that the size of Ag NPs changed little. The results revealed that **L** was a very important factor in determining the size of Ag NPs in this work. Clearly, an optimum particle size should exist to balance the appropriate bandgap and couple with **L**.
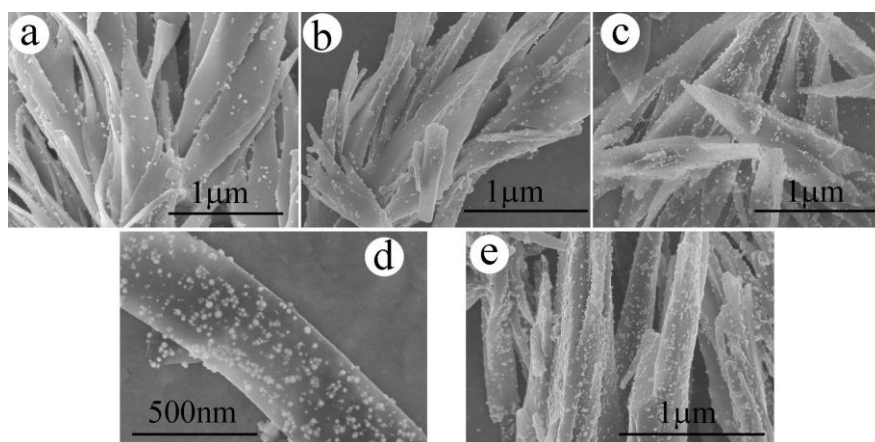

Figure S12. SEM images of the as-prepared products at various concentration of AgNO$_3$:

(a) **L**: Ag = 5:1; (b) **L**: Ag = 2:1; (c) **L**: Ag = 1:3; (d) **L**: Ag = 1:5; (e) **L**: Ag = 1:10.
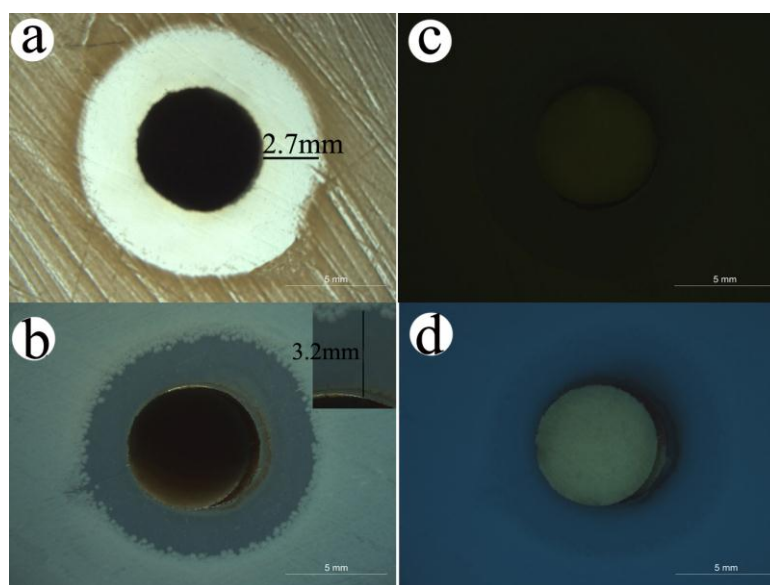
Fig. S13 Photograph images of the zone of inhibition of *S. aureus.* (a)-(b) bright-field image of **L** and **L**/Ag nanohybrids, respectively; (c)-(d) fluorescence microscopy of (a)-(b) respectively.
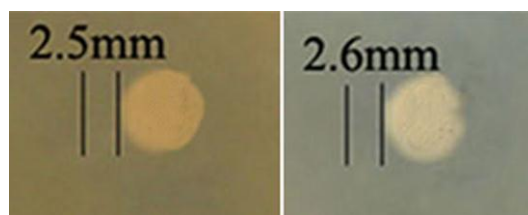

Fig S14 Photograph images of the zone of inhibition of Ag NPs for *S. aureus* (laft) and *E. coli* (right)
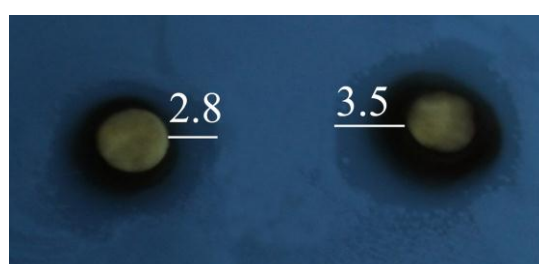

Fig S15 Photograph images of the zone of inhibition of the mixture physically mixed **L** nanofibres and Ag NCs for *S. aureus* (left) and *E. coli* (right)
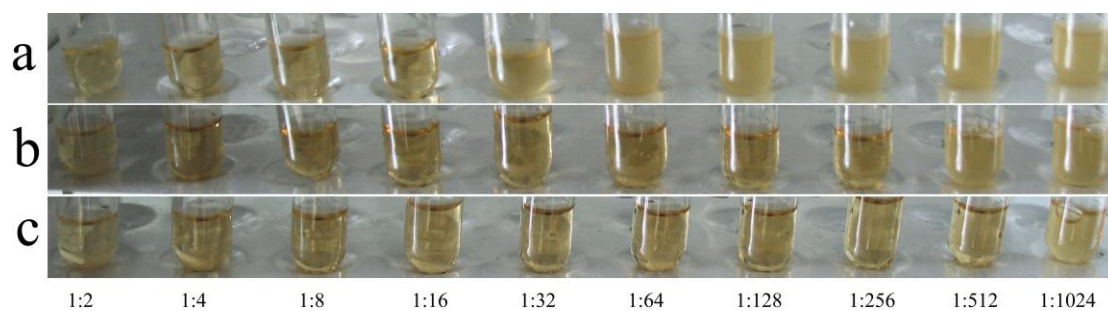
MIC of Antibacterial Effect

Figure S16 Antibacterial effect of (a) **L** (b) Ag (c) **L**/Ag nanohybrid

Reference

S1 D. H. Yu, J. Q. Wang, L. Kong and Z. D. Liu, 10-Ethyl-10H-phenothiazine-3-carbaldehyde,

Acta Crystallographica Section E, **2011**, *E67*, o3344.